Supporting Information

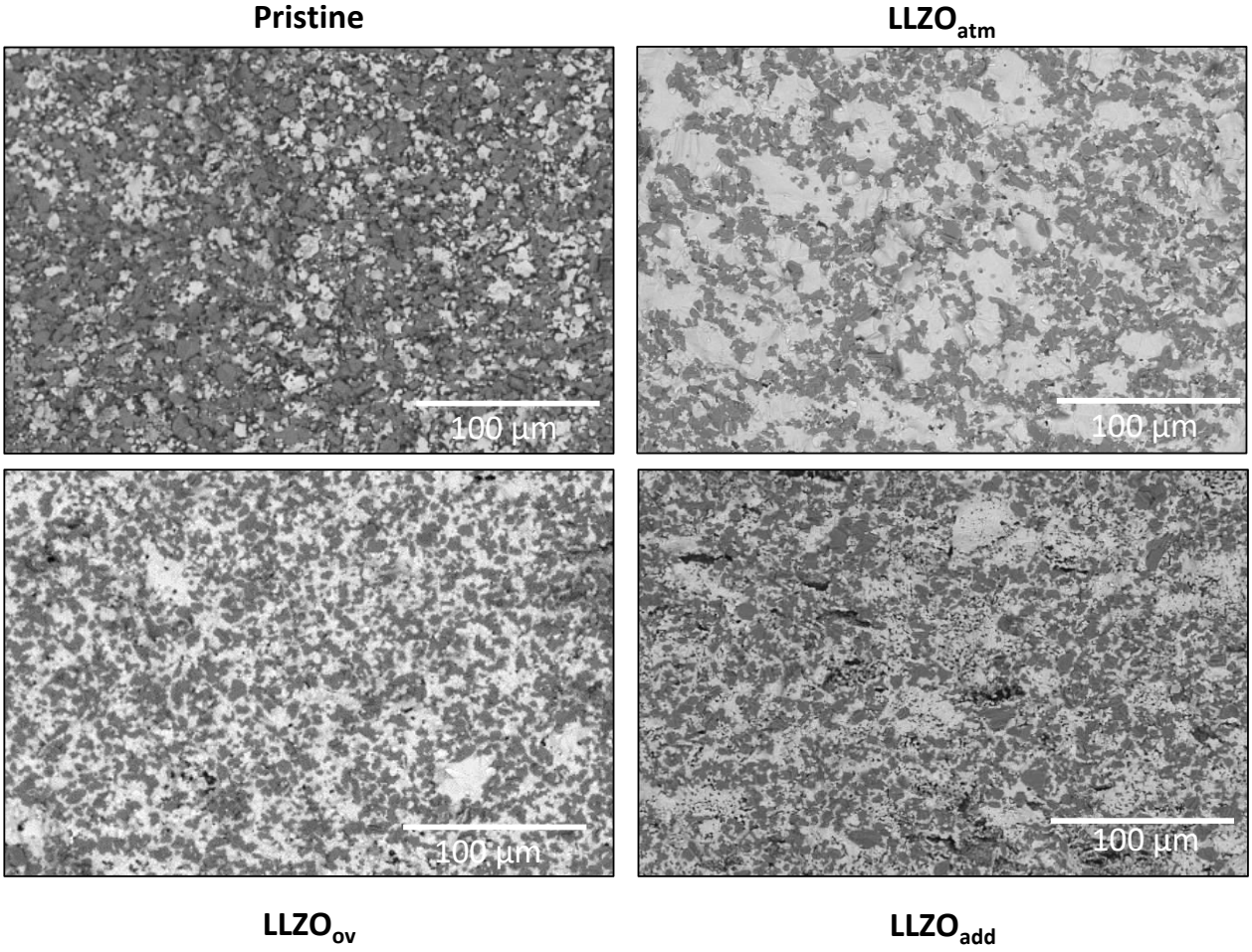

S 1 Cross-sectional SEM images of fractured pristine (upper left), $LLZO_{atm}$ (upper right), $LLZO_{ov}$ (lower left), and $LLZO_{add}$ (lower right) samples.

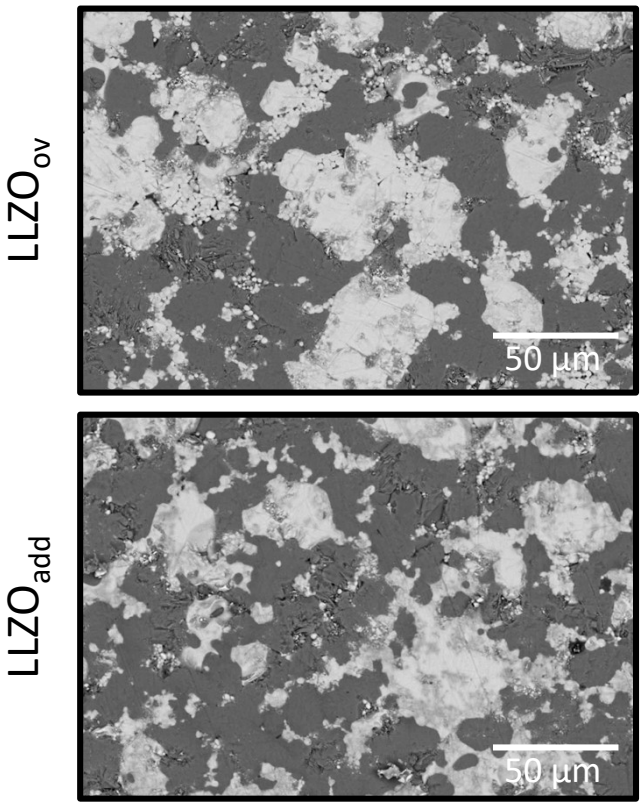

S 2 Higher magnification fractured SEM cross-section images of LLZO/LCO cathodes.

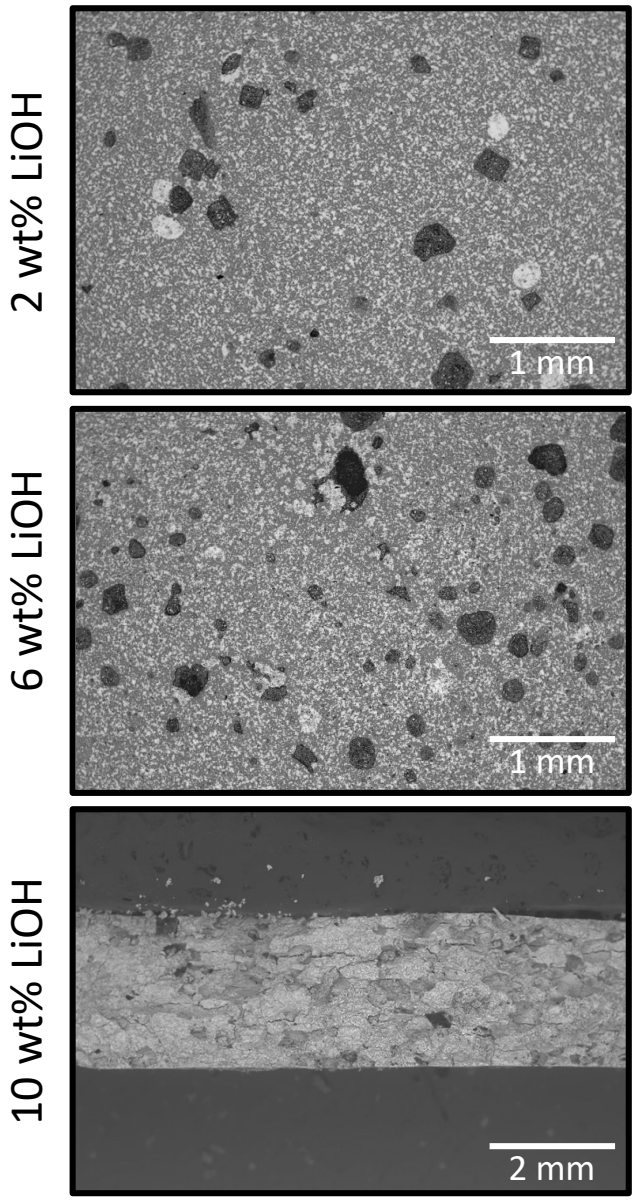

S 3 Addition of 2, 6 and 10 wt% LiOH to LLZO/LCO composite cathodes. 10 wt% LiOH addition led to cracked and mechanically instable pellets.

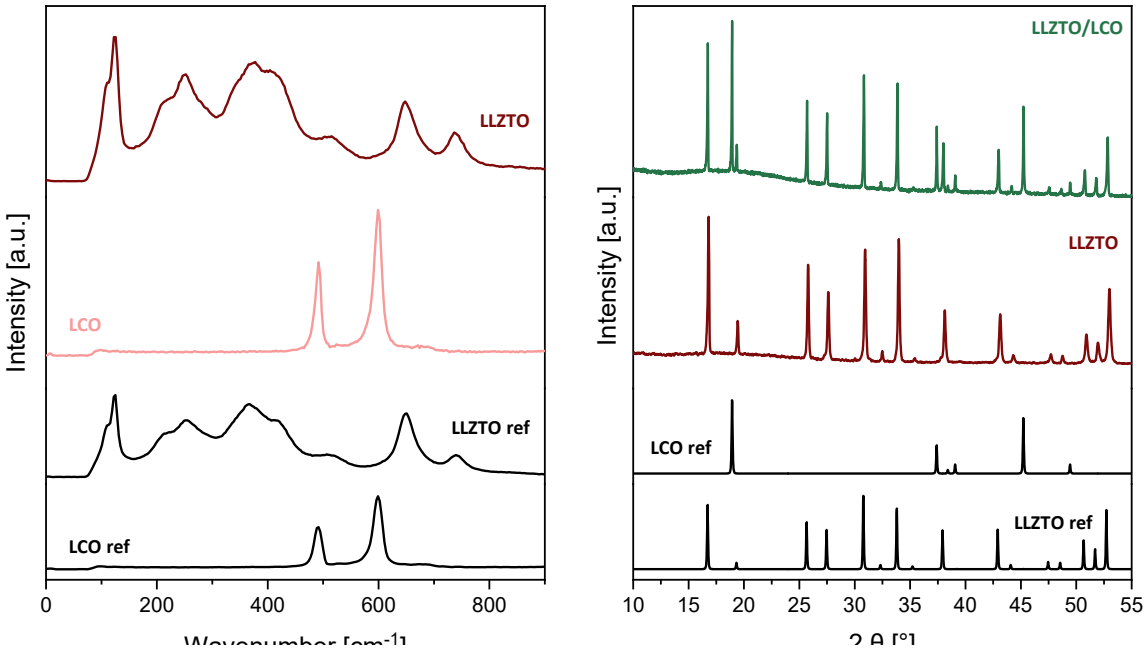

S 4 Raman spectra (left) and XRD diffractograms (right) of as-synthesized LLZO and commercial LCO.

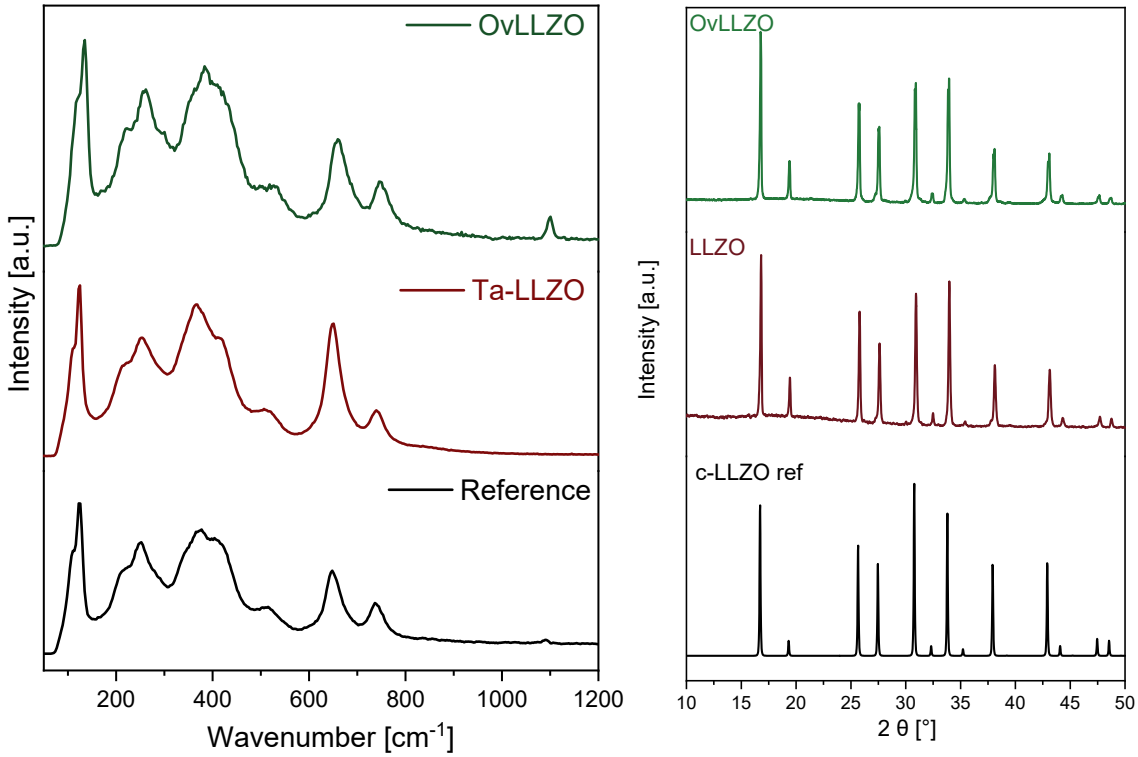

S 5 Raman spectra (left) and XRD diffractograms (righ) of as-synthesized overlithiated LLZO.

Compound	LLZO			LCO		
Lattice parameter	a	b	c	a	b	c
Pristine LLZO-LCO before sintering	12,9481	12,9481	12,9481	2,8159	2,8159	14,0545
Pristine LLZO-LCO after sintering	12,9502	12,9502	12,9502	2,81858	2,81858	14,0711
As-synthesized Overlithiated LLZO	12,951	12,951	12,951	-	-	-
As-sintered LCO-LLZO$_{add}$	12,94275	12,94275	12,94275	2,81481	2,81481	14,04362
As-sintered LCO-LLZO$_{ov}$	12,94759	12,94759	12,94759	2,81434	2,81434	14,04493
As-sintered LCO-LLZO$_{atm}$	12,94243	12,94243	12,94243	2,8151	2,8151	14,04766

Fit Parameter	R_p	R_{wp}	R_{exp}
Pristine LLZO-LCO before sintering	3.47	4.21	2.02
Pristine LLZO-LCO after sintering	4.93	4.11	3.24
As-synthesized Overlithiated LLZO	4.07	5.39	2.71
As-sintered LCO-LLZO$_{add}$	5.00	5.13	2.66
As-sintered LCO-LLZO$_{ov}$	3.98	4.60	3.19
As-sintered LCO-LLZO$_{atm}$	4.45	4.21	2.46

S 6 Lattice parameters from Rietveld refinements and fit parameters.

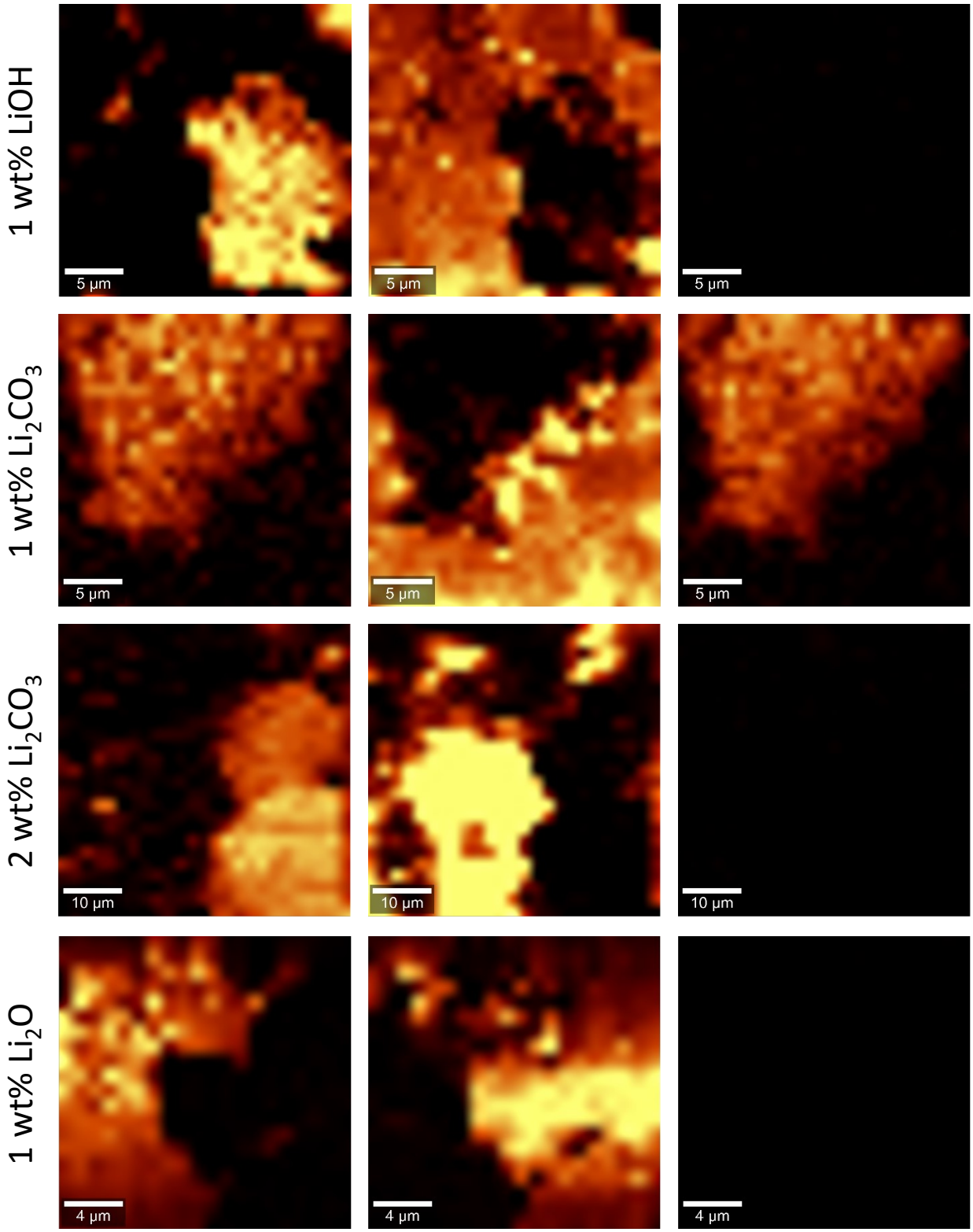

S 7 Raman mapping of different lithium-containing additives in LLZO/LCO composite cathode pellets.

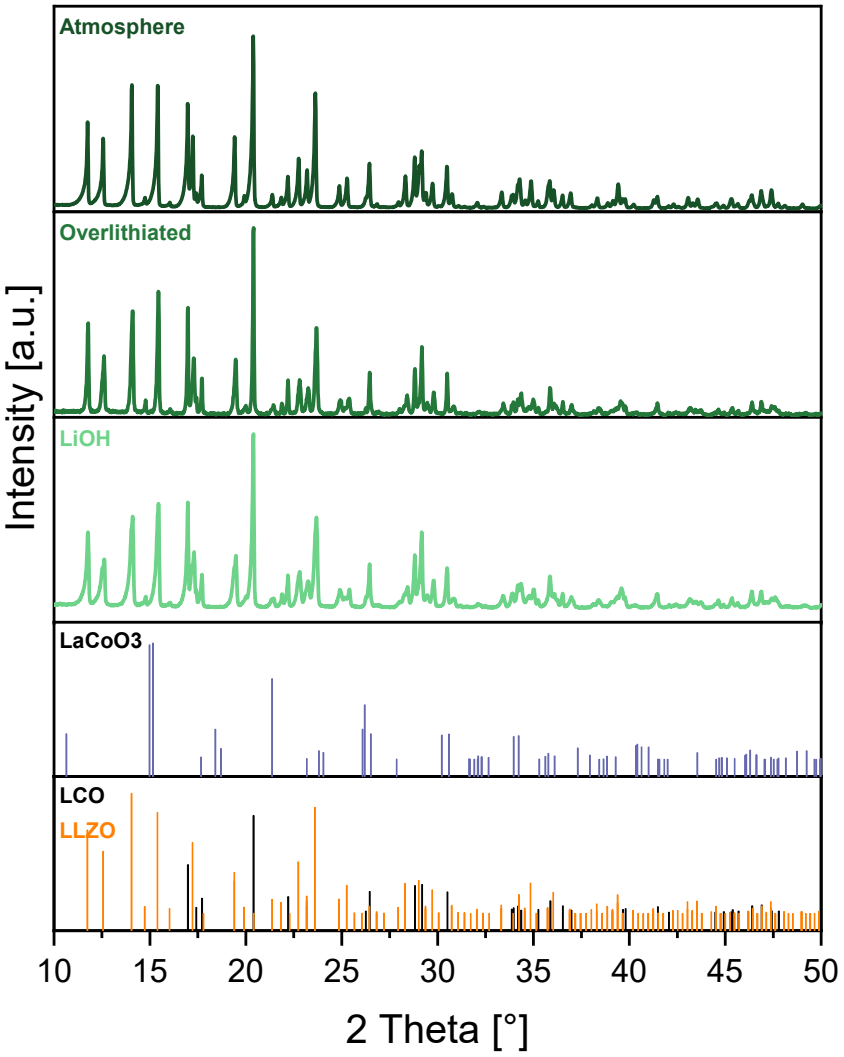

S 8 XRD Diffractograms of composite cathode tapes.

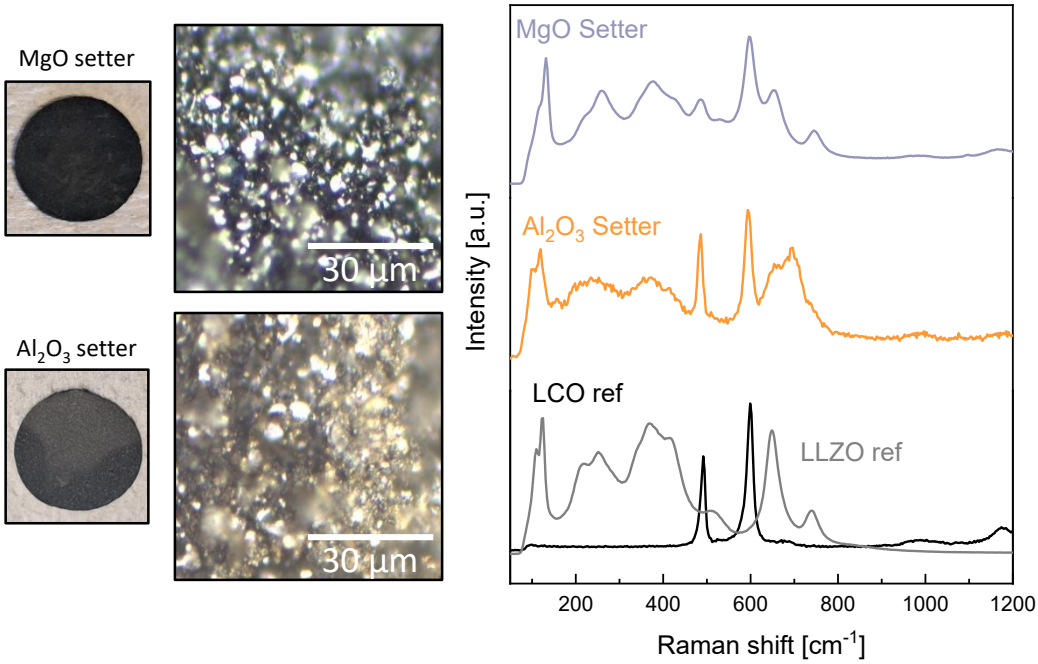

S 9 Difference of setter plates on chemical stability. Left: Optical pictures of tapes. Middle: Microscopy picture of tapes - yellow discoloration is indicative of secondary phase formation. Right: Averaged Raman spectra of both tapes co-fired in between different setter plates.

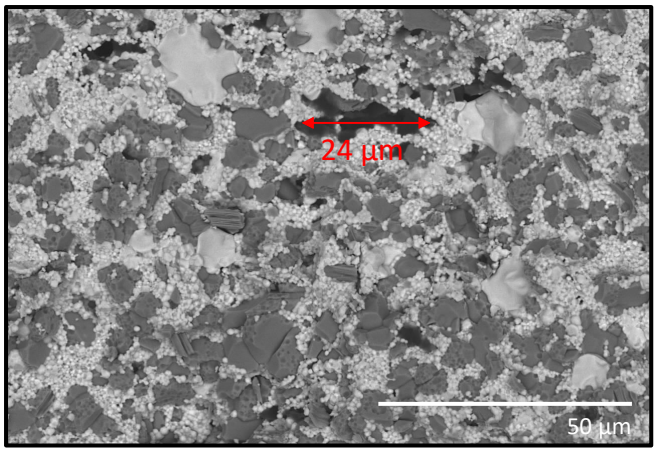

S 10 Magnified SEM image of an LCO-LLZO$_{add}$ tape with large pore.

	PEO	LCO-LLZO$_{atm}$	LCO-LLZO$_{add}$	LCO-LLZO$_{Ov}$
Resistance [Ohm cm^2]	1406	1601	1649	1669
Difference [Ohm cm^2]		195	243	263
Conductivity [S cm^{-1}]	2,13371E-06	6,15385E-05	4,93827E-05	4,56274E-05

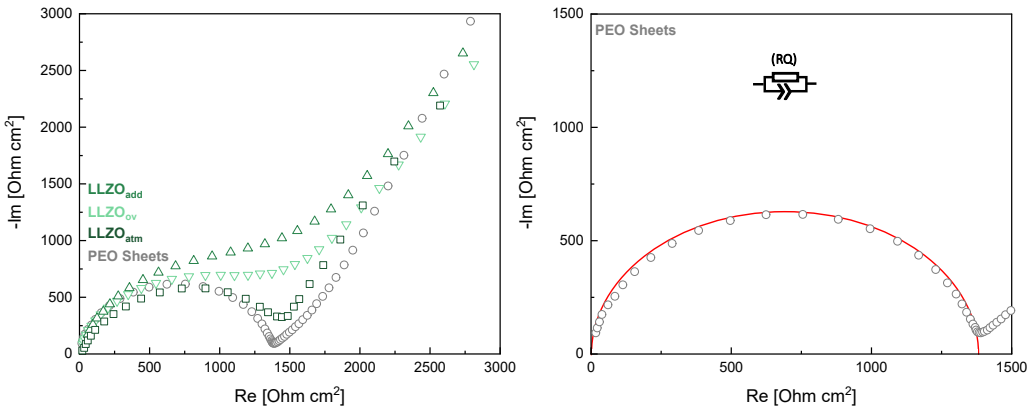

S 11 Top: Resistance and calculated ionic conductivity values. Bottom: Fit for High-frequency semicircles.

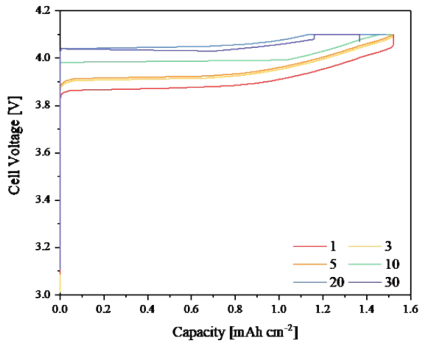

Cycle	Coulombic efficiency (Qdis/Qchg)
1	99.2%
3	101.3%
5	98.8%
10	96.5%
20	92.3%
30	95,4%

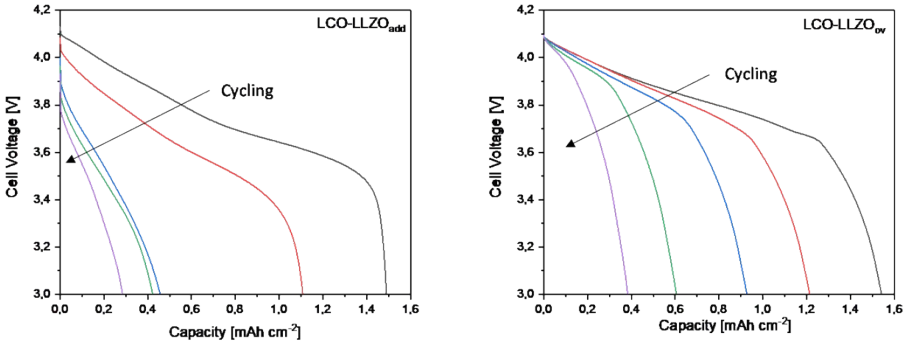

S 12 Top: Charge capacity plots for LCO-LLZO$_{atm}$ (left) and Coulombic efficiency for selected cycles (right). Bottom: Cell Voltage over discharge capacity plot for LCO-LLZO$_{add}$ (left) an LCO-LLZO$_{ov}$ (right)

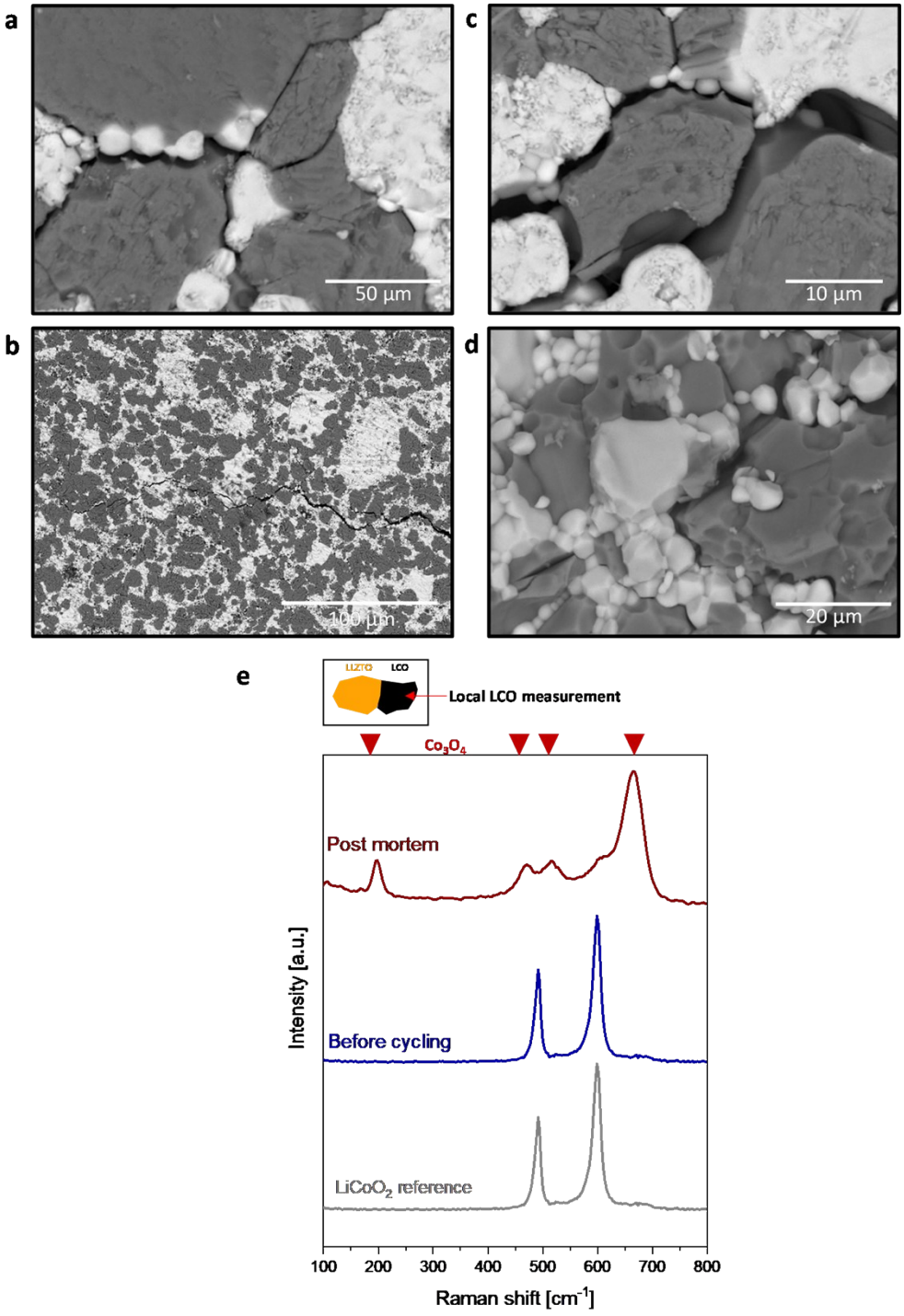

S 13 Post-mortem analysis of the lithium-compensated batteries. A+C+D) SEM picture of interfacial cracks between LLZO and LCO due to volume exchange of LCO as well as intergranular LCO and LLZO cracking. B) SEM picture of larger cracks propagating several hundreds of microns throughout the cathode. E) Raman spectra of locally measured LCO particles before and after cycling.

Sample	Active material loading [mg_{LCO} cm^{-2}]	Gravimetric capacity [mAh g_{LCO}^{-1}]	Area specific capacity [mAh cm^{-2}]
LCO-LLZO$_{atm}$	11.4	136	1.55
LCO-LLZO$_{add}$	11.4	131	1.49
LCO-LLZO$_{Ov}$	11.4	135	1.54

S 14 Comparison of cathode loadings and capacities for all three cells